Available online at www.sciencedirect.com
ScienceDirect
Journal of Membrane Science 288 (2007) 20–27
journal of MEMBRANE SCIENCE
www.elsevier.com/locate/memsci

Co-sintering synthesis of tubular bilayer α-alumina membrane

Jun Feng, Yiqun Fan, Hong Qi, Nanping Xu *

Membrane Science & Technology Research Center, Key laboratory of Material-oriented Chemical Engineering of Jiangsu Province and MOE, Nanjing University of Technology, Nanjing 210009, China

Received 7 April 2006; received in revised form 19 September 2006; accepted 20 September 2006
Available online 24 September 2006

Abstract

In order to reduce production time and costs, a co-sintering process was proposed to prepare tubular bilayer α-alumina membrane. The shrinkage mismatch between two membrane layers during co-sintering was the first problem to be solved. The selection of the co-sintering temperature was the main issue addressed in this paper. Experimental results showed that too large mismatch in the sintering shrinkage of two membrane layers could cause defects such as cracks and big pores while moderate shrinkage mismatch between two membrane layers during co-sintering was beneficial. SEM images of the membrane prepared by co-sintering at 1300 °C showed that the membrane surface was defect-free and the interfacial bonding was good. Ultrasonic treatment did not damage the microstructure and the permeability of the membrane synthesized by co-sintering at 1300 °C. The filtration of the $CaCO_3$ suspension showed that the membrane treated by co-sintering had a higher steady permeate flux than the membrane prepared by conventional process and can withstand a high back-flushing pressure.

Keywords: Co-sintering; α-Alumina; Ceramic membrane

1. Introduction

Conventionally, a multilayer ceramic membrane can be obtained by repeating the coating procedure, usually including the costly heat treatment after each coating [1]. To reduce the costs of production in industry, co-sintering technique has attracted much attention. As an economic fabrication method for multilayer structures, co-sintering has been researched in many fields such as ceramic membranes [2–4], electronic packages, especially low-temperature co-fired ceramics (LTCC) [5] and solid oxide fuel cells (SOFC) [6–8]. The thermal mismatch of each layer is a common and key problem during the co-sintering process. In a multilayer ceramic membrane, each membrane layer, which is made from ceramic powders with different compositions and particle sizes, exhibits different sintering behaviors. Therefore, it is important that the co-sintering process should ensure the sufficient sintering of each membrane layer and also ensure the high bonding strength of each membrane layer in an asymmetric ceramic membrane.

Lindqvist and Liden [2] reported the preparation of a flat α-alumina microfiltration membrane by tape-casting of the support and the membrane, followed by lamination by high pressure and sintering in one step. However, in order to co-sinter the support with the first membrane layer, they decreased the sintering temperature of the support at the cost of mechanical strength. The interface between the support and the membrane layer was only examined by SEM without further characterizations. Jong et al. [4] investigated the single-step synthesis of bilayer α-alumina hollow fibers based on co-sintering heat treatment. They highlighted the position of the separation layer, which comprised smaller particles compared to the support layer. The outer separation layer had a larger shrinkage rate compared to the inner support layer and therefore the outer layer could bind the inner layer tightly during the co-sintering process. However, the mechanical strength of the whole fiber after co-sintering was poor. The bonding strength between two layers was only confirmed by breakage the fibers without separation of the two layers and SEM images. The present study is aimed to prepare a tubular bilayer α-alumina membrane on a rigid Al_2O_3 support by a co-sintering process. It is different from most other co-sintering processes which co-sinter multilayer structures without additional rigid substrates. In this paper, the co-sintering fabrication and characterization of bilayer α-alumina

* Corresponding author. Tel.: +86 25 83587174; fax: +86 25 83300345.
E-mail address: npxu@njut.edu.cn (N. Xu).

0376-7388/$ – see front matter © 2007 Elsevier B.V. All rights reserved.
doi:10.1016/j.memsci.2006.09.034

membranes are addressed and the co-sintering temperature is optimized.

2. Experimental

2.1. Powder characterization

Two α-alumina powders, which were referred as A1 and A2, were used in this work. The average particle size and the size distribution were determined using Mastersizer 2000 (Malvern, UK). The size distribution can be seen in Fig. 1. All the powders were used without further pre-treatments. Powder A1, with an average particle size of 2.1 μm and specific surface area of 3.8 m^2/g, was used to prepare the sub-layer membrane. Powder A2, with an average particle size of 1.0 μm and specific surface area of 7.5 m^2/g, was used to fabricate the top-layer membrane.

2.2. Fabrication of bilayer α-alumina membranes by co-sintering process

Stable coating slurries were prepared with two α-alumina powders, respectively. The α-alumina powders were dispersed into pure water with 6 vol.% nitric acid (1 mol/L) as a dispersant and stirred for 3–5 h to prepare coating slurries with solid contents of 23 and 15 wt.% for the sub-layer and the top-layer membrane, respectively. Optical microscopy was used to determine that all the agglomerates had been broken down. Next, methylcellulose (MC) was added, as binder, to the slurry and stirred for another 30 min. After degassing under vacuum, the slurry was ready for dip-coating. The viscosities of the slurries for the sub-layer and the top-layer membrane were about 4.5×10^{-3} and 3×10^{-3} Pa s, respectively, measured by rotary viscosimeter (DV-II+, Brookfield Engineering Labs., Inc., USA) at 30 °C.

The supports used were tubular α-alumina supports (12 mm in outer diameter, 85 mm in length and 2 mm in wall thickness) made by our Membrane Science and Technology Research Center (Nanjing, China). Before use, the supports were cleaned with acetone and dried at 150 °C to remove surface dirt and grease. The treated support was brought into the slurry made from A1 for 30–90 s and subsequently withdrawn from the slurry. The wet membrane was dried overnight at room temperature. After repeating the coating procedure with the slurry made from A2 for 30–60 s, the supported bilayer membrane was dried overnight at room temperature and at 120 °C for 5 h. Membranes were co-sintered at 1450, 1300 and 1250 °C, respectively, for 2 h with the heating and cooling rate of 2 °C min^{-1} in an electric furnace.

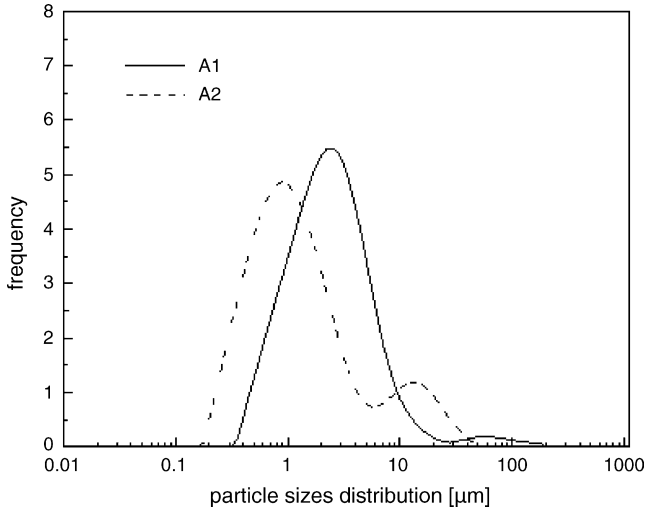

Fig. 1. Particle size distribution of two α-Al_2O_3 powders used in this investigation (A1 was used to prepare the sub-layer membrane, A2 was used to fabricate the top-layer membrane).

In order to check the properties of membranes made by different processes, we also prepared tubular bilayer α-alumina membranes by a conventional process with the same slurries and the same soaking time during dip-coating. During the conventional preparation process, the sub-layer and the top-layer membranes were sintered at 1450 and 1300 °C, respectively, which were the suitable sintering temperature of each membrane layer, as revealed by experimental optimization.

2.3. Dilatometry

A differential thermal dilatometer (DIL402C, Netzsch, German) was used to study the shrinkage behaviors of the membrane layers during sintering. The shrinkage rate ($\Delta l/l_0$) was measured under temperature-rising conditions and the sample temperature was raised to 1450 °C at an increase rate of 2 °C min^{-1}.

2.4. Characterization of bilayer α-alumina membranes

Section morphologies of the synthesized membranes were analyzed by scanning electron microscopy (SEM) (Quanta 200, Philip, USA).

Average pore size and pore size distribution (PSD) of the membranes were measured by the gas bubble pressure method (GBP), which was performed following the American Society for Testing and Materials (ASTM) Publication (F316-80). All samples were immersed in isobutyl alcohol for 3 h under vacuum. During the process of measurement, the flow rate and the trans-membrane pressure of nitrogen were measured.

The membrane porosity was estimated from the corresponding unsupported membrane treated under the same condition by mercury porosimetry (Poremaster GT-60, Quantachrome, USA).

Pure water flux (PWF) of the membrane was measured in a cross-flow filtrating apparatus illustrated in Fig. 2. The apparatus was capable of operating at a variety of temperatures and pressures. The membranes were saturated with pure water (conductivity: 4.5 μs/cm) before the pressure was applied to avoid non-stationary transient effects [9]. The effective filtration area was 2.14×10^{-3} m^2 for all samples. PWF of the membrane was determined by collecting the permeation in a graduated cylinder and timing the collection period.

The separation property was tested by the same apparatus. Moreover, a high-pressure back-flushing was introduced in the cross-flow filtration. The $CaCO_3$ (average particle size 0.4 μm) suspension with a mass content of approximately 3 g/L was used

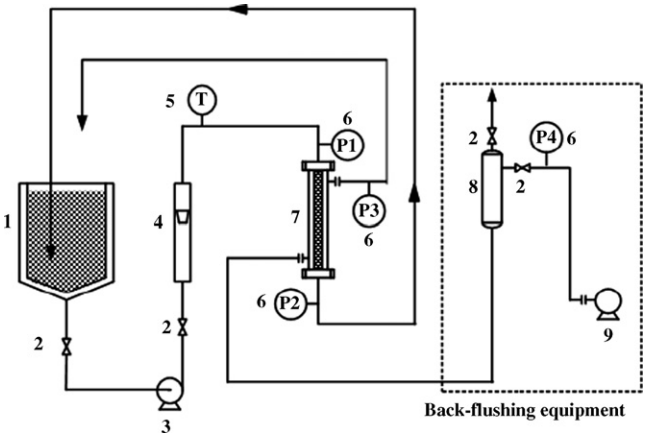

Fig. 2. Schematic of cross-flow filtration apparatus with back-flushing equipment: (1): feed tank; (2): needle valve; (3): centrifugal pump; (4): flow meter; (5): temperature meter; (6): pressure gauge; (7): membrane module; (8): buffer tank; (9): air compressor.

in the cross-flow filtration experiments. The operation pressure was maintained at 0.1 MPa and the cross-flow velocity was kept at 3 m s^{-1}. Both permeate and retentate were recycled back to the feed tank to maintain the concentration of the feed. The permeate flux was determined by the same method as PWF. When the permeate flux reached a stable value, an intermittent back-flushing pressure was applied to dislodge $CaCO_3$ particles trapped on and in the membrane surface. In general, the back-flushing pressure should be more than twice the forward filtration pressure [10,11]. In this work, the back-flushing pressure was fixed at 0.5–0.6 MPa with duration of 5 s.

3. Results and discussions

3.1. Sintering behaviors of the membrane layers

3.1.1. Shrinkage characteristics of α-alumina

In order to study the sintering behaviors of each membrane layer during co-sintering and conventional processes, we prepared two unsupported membranes, which were prepared on plaster supports and separated from the supports before sintering. The "green" unsupported membrane was referred to as M1, which was made from A1 without sintering, and M2, which was made from A2 without sintering.

The shrinkage behaviors of M1 and M2 are shown in Fig. 3. It reveals that the two "green" membranes begin to shrink at about 1000 °C. Compared to M1, M2 has a larger shrinkage rate from approximately 1000 to 1450 °C and the shrinkage curve of M2 is very sharp with a final shrinkage rate of approximately 16% at 1450 °C.

3.1.2. Stress state of the membrane layers during sintering

To analyze the stress state of the membrane layers during sintering and co-sintering processes in a simple way, we regarded the ceramic support or the sintered membrane layer as a rigid substrate [12–14]. In the conventional process, each membrane layer is dip-coated on a support or a sintered membrane layer. Therefore, the shrinkage of each membrane layer during sintering is constrained by a rigid substrate perpendicularly and consequently the substrate exerts a tensile stress on the membrane [12–14].

During the co-sintering process, the "green" sub-layer and the "green" top-layer membranes are bonded together and must shrink at the same rate. Thus, the application of co-sintering becomes complicated considering the difference in shrinkage rates between the two membrane layers, which can be seen from Fig. 3. It is difficult to evaluate the exact values of the sintering mismatch stresses, but the shrinkage curves obtained by dilatometry can give a useful measure of the stresses as a result of sintering mismatch during the co-sintering process [15,16]. Accordingly, the difference in the shrinkage rate between two membrane layers can cause a tensile stress in the top-layer membrane and compressive stress in the sub-layer membrane [7,15–18]. Meanwhile, the sub-layer membrane is subjected to a tensile stress resulting from the support below. In our experiment, we determined the relative magnitude of sintering stress qualitatively by the degree of mismatch in sintering shrinkage rates. The differential shrinkage rate between the sub-layer membrane and the support is equal to the shrinkage rate of the sub-layer membrane since the support can be regarded as a rigid substrate. We can see from Fig. 3 that the differential shrinkage rate between the two membrane layers is always larger than the differential shrinkage rate between the sub-layer membrane and the support from 1000 °C to 1450 °C. Therefore, the sub-layer membrane is completely in a state of compressive stress caused by the top-layer membrane during the co-sintering process. The stress state of each membrane layer during the

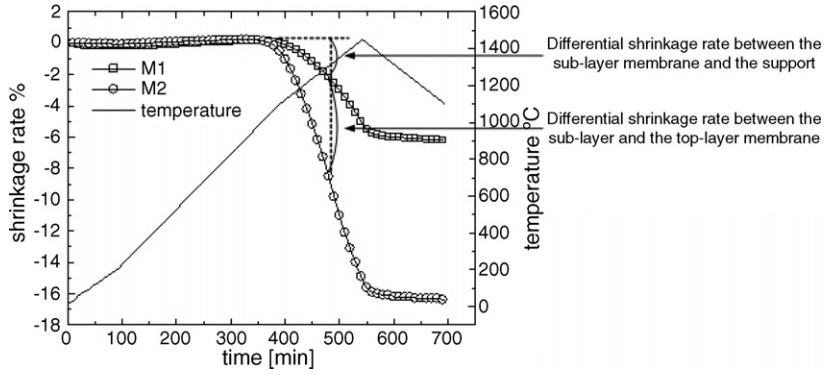

Fig. 3. Dilatometric shrinkage curves of M1 and M2.

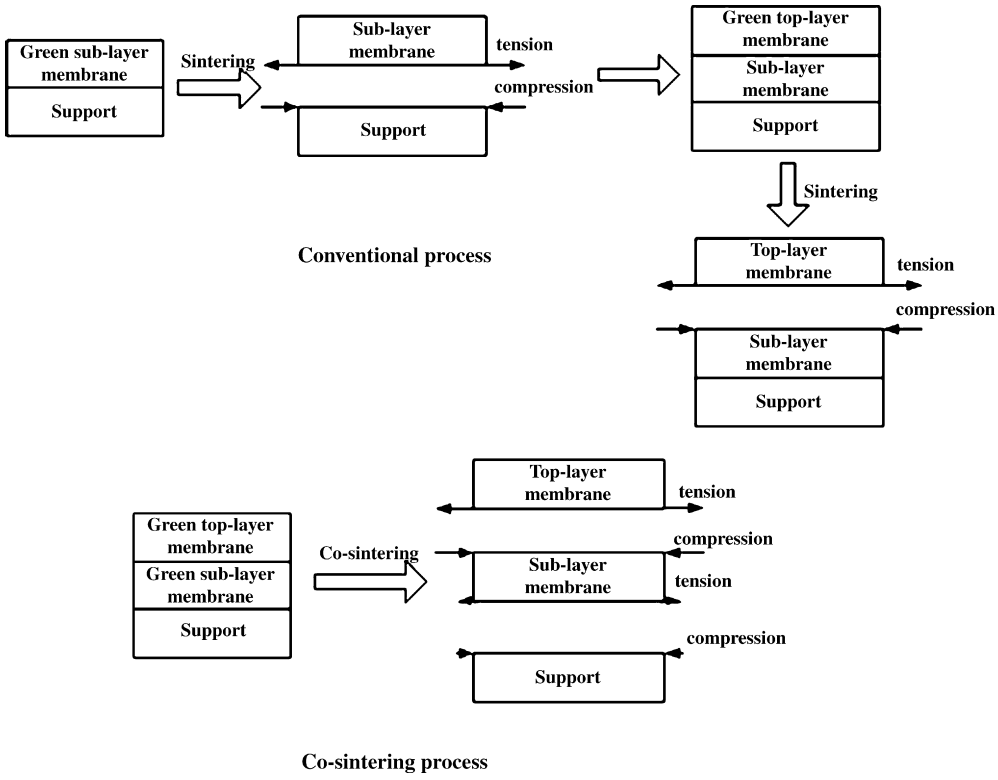

Fig. 4. The stress state of each membrane layer during conventional and co-sintering process.

conventional and the co-sintering processes is illustrated in Fig. 4.

3.2. Co-sintering synthesis of bilayer membranes

The study was mainly focused on the optimization of co-sintering temperature although the thickness of each membrane layer is another important factor during the co-sintering process, which will be investigated in the near future. In this work, the thickness of the sub-layer and the top-layer membrane were controlled to 20–30 and 10–15 μm, respectively, by adjusting the binder content in the coating slurry. Here, co-sintering was first carried out at two specific temperatures 1450 and 1300 °C, which are the suitable sintering temperatures of the sub-layer and the top-layer membrane during the conventional process, respectively.

3.2.1. Co-sintering at 1450 °C

It was expected that co-sintering at 1450 °C would ensure sufficient sintering of the double membrane layers and also high bonding strength between the double membrane layers and the support. However, many defects occurred after co-sintering at 1450 °C, which can be clearly seen in Fig. 5 (a and b). The average pore size estimated from GBP is about 0.31 μm, which is shown in Fig. 6. The defects must have formed as a result of quite a large degree of shrinkage mismatch between the two membrane layers during co-sintering at 1450 °C. From Fig. 3 it can be seen that M2 has a much larger shrinkage rate, which is about 16% compared to only 6% shrinkage rate of M1 at 1450 °C. Lindqvist and Liden [2] had also observed the same phenomenon.

3.2.2. Co-sintering at 1300 °C

Fig. 7 (a–c) present morphologies of bilayer membrane fabricated by co-sintering at 1300 °C. Fig. 7 (a and b) reveal that the surface is homogeneous and smooth without defects. Fig. 7 (c) illustrates the excellent interface with good adherence and nearly no penetration between each membrane layer. The average pore size estimated from GBP is about 0.20 μm with a narrow pore size distribution, which can be seen from Fig. 8 (b). The relation between the flow rate of nitrogen through the dry and the wet membrane is shown in Fig. 8 (a). The flow rate of nitrogen through the wet membrane increases with higher pressure, followed by a sharp increase when the pressure is increased to 0.48 MPa, for the most frequent pore of the synthesized bilayer membrane is opened.

Experiments showed that the single sub-layer membrane sintered at 1300 °C peeled off from the support easily. The result of dilatometry also showed that the shrinkage rate of M1 at 1300 °C was only 2%. However, when the sub-layer membrane was sintered together with the top-layer membrane, it sintered effectively. The beneficial influence of the compressive stress on the sintering of the sub-layer membrane, which is exerted by the faster shrinkage of the top-layer membrane during co-sintering, is thought to play an important role in this process. It is well known that compression is a beneficial factor to sinter-

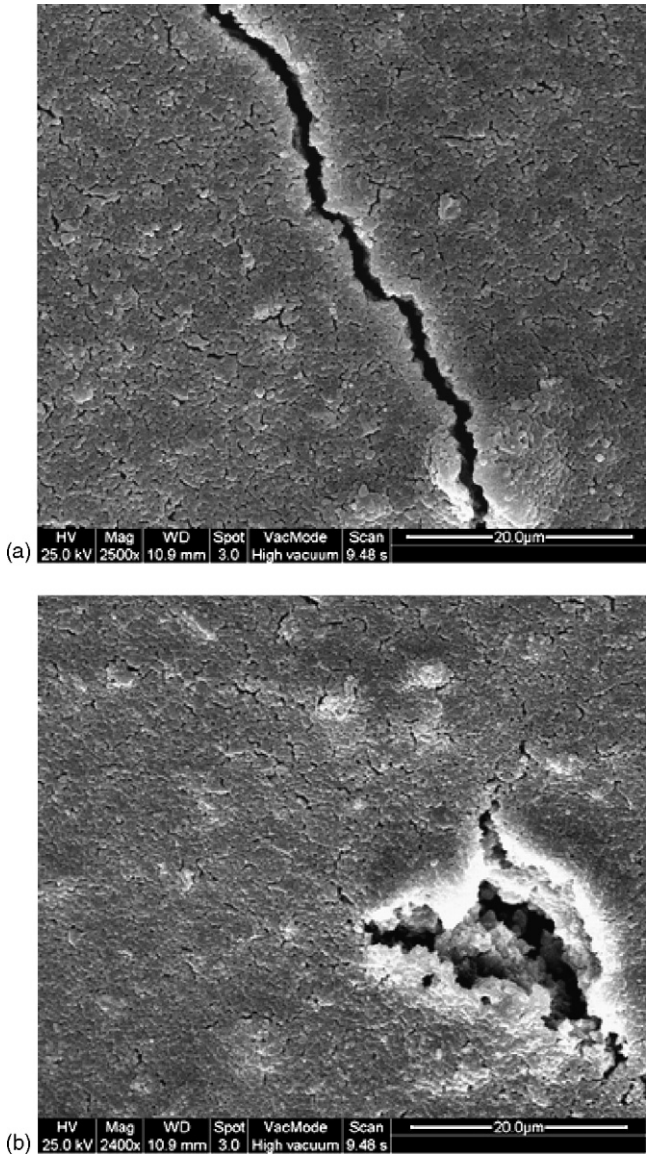

Fig. 5. The surface morphology of bilayer α-Al_2O_3 membrane co-sintered at 1450 °C; (a) crack and (b) big pore.

ing [18–20]. In addition; the sintering mismatch between two membrane layers is reduced by decreasing the co-sintering temperature from 1450 to 1300 °C. Therefore, the defects, which occurred when co-sintering at 1450 °C, did not occur when co-sintering at 1300 °C.

Furthermore, we co-sintered the bilayer membrane at 1250 °C for 2 h. Owing to the insufficient sintering of the sub-layer membrane at such a low-temperature compared with the suitable sintering temperature (1450 °C) for conventional process, the prepared bilayer membrane peeled off from the support easily. Co-sintering of the bilayer membrane at some temperature between 1300 and 1450 °C might also prepare a defect-free bilayer membrane with high bonding strength but as long as the produced membranes have sufficient mechanical strength for practice, the lower co-sintering temperature is appreciated.

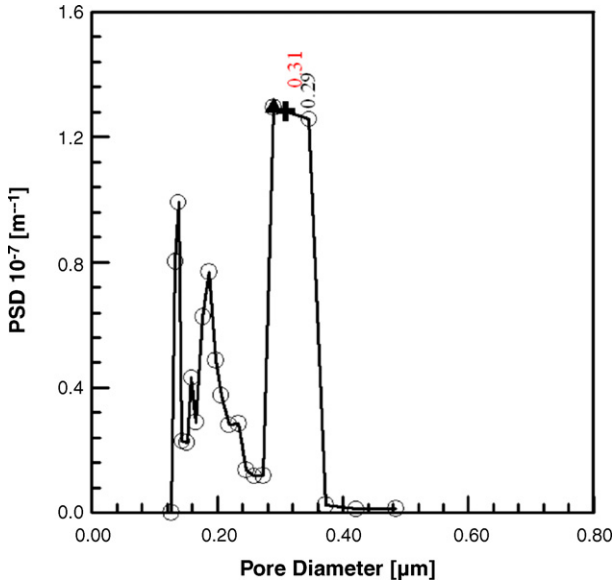

Fig. 6. Pore size distribution (◯) of the bilayer α-Al_2O_3 membrane co-sintered at 1450 °C; the most frequent pore size (+) and the average pore size (▲).

3.3. Permeability measurements

Fig. 9 shows the PWF of the bilayer membrane prepared by the co-sintering and the conventional process. All experiments were repeated three times for each set of conditions and the results presented here are the average values. The results show that the bilayer membranes formed by the co-sintering process exhibit a much higher PWF than the ones derived from the conventional process with the same slurries and the same soaking time during dip-coating. The main reason for this higher PWF of the membrane made by the co-sintering process is the different thickness of the top-layer membrane. Before coating the top-layer membrane, the "green" sub-layer membrane in the co-sintering process contains more organic additives and physically absorbed water, so the capillary action of it is weaker than the sintered sub-layer membrane in the conventional process. With weaker capillary action under the same soaking time, a thinner top-layer membrane was obtained by the co-sintering process [1]. For comparison, the cross-section morphology of the bilayer α-alumina membrane made by the conventional process is showed in Fig. 10. The difference in the top-layer membrane thickness can be seen clearly from Figs. 10 and 7(c). On the other hand, the porosity of the sub-layer membrane increases when co-sintering at 1300 °C. Many researchers have proven the relation between the porosity of the membrane and the corresponding sintering temperature [2,21]. To confirm the change of porosity in the sub-layer membrane, the unsupported sub-layer membranes sintered at 1300 and 1450 °C were studied by mercury porosimetry. The porosity is 53.9% and 41.5% after sintering at 1300 and 1450 °C, respectively. The results demonstrate that the corresponding porosity of the sub-layer membrane might increase with sintering temperature reducing from conventional 1450 to 1300 °C. In addition, it should be pointed out that due to the existence of defects and larger average pore sizes, the bilayer membrane co-sintered

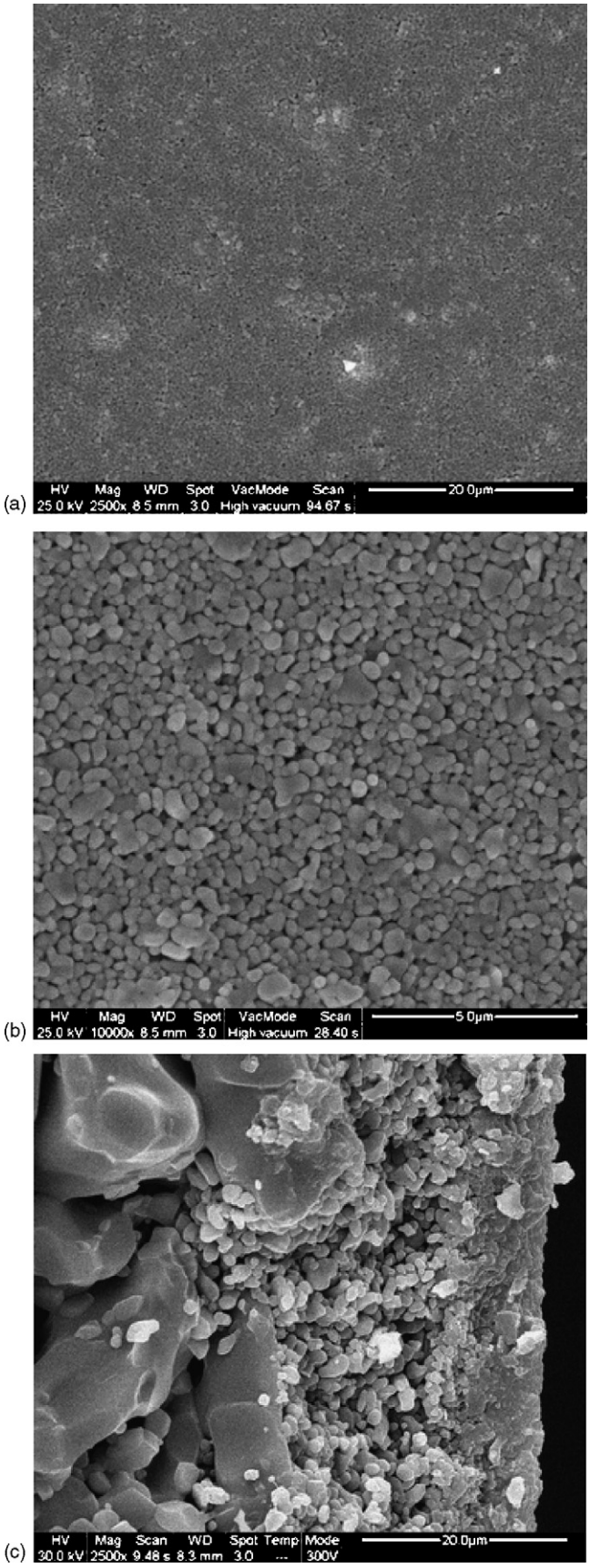

Fig. 7. The morphology of bilayer α-Al_2O_3 membrane co-sintered at 1300 °C: (a) surface image 2500×; (b) surface image 10,000×; (c) cross-section image.

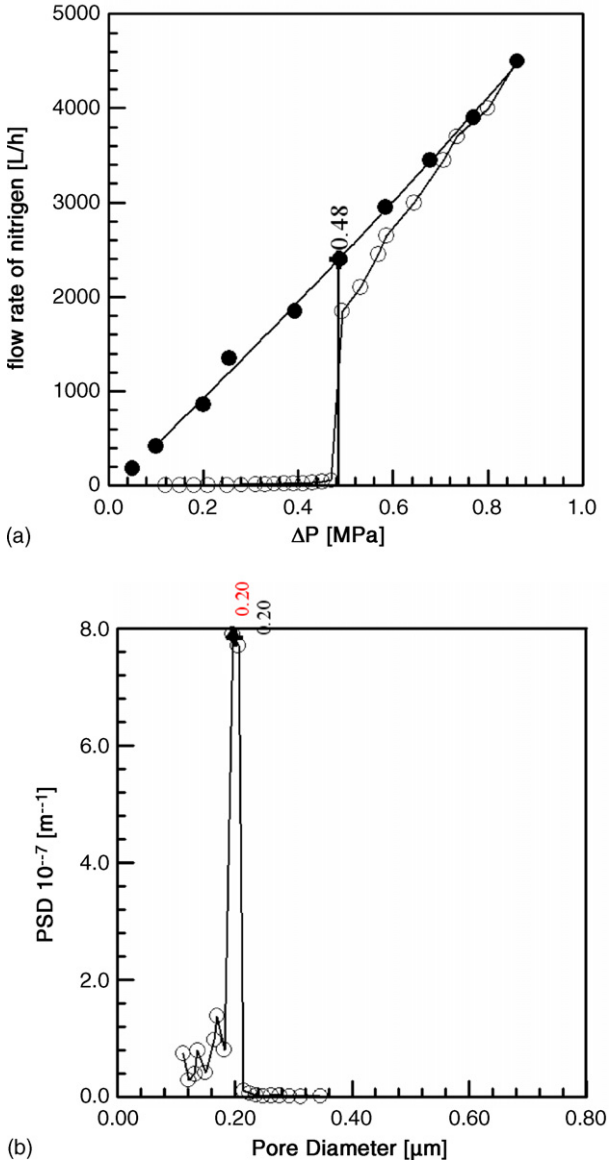

Fig. 8. (a) The flow rate of nitrogen through the wet (◯) and the dry (●) bilayer α-Al_2O_3 membrane co-sintered at 1300 °C, (+) pressure to open the most frequent pore; (b) pore size distribution (◯) of the bilayer α-Al_2O_3 membrane co-sintered at 1300 °C, the most frequent pore size (+), the average pore size (▲).

at 1450 °C has a slight higher PWF than that co-sintered at 1300 °C.

Different from the bilayer hollow fiber co-sintered by Jong et al. [4], the top-layer membrane, which was dip-coated in the innermost layer, shrank faster than the outer sub-layer membrane. Therefore delamination was easier to happen in our co-sintering process. To further evaluate the bonding strength of the bilayer membrane formed by co-sintering at 1300 °C, the prepared membranes were subjected to ultrasonic vibrations (160 W, 40 KHz) for 30 min for three times. The average pore size and PWF tested before and after ultrasonic treatment are given in Table 1. It illustrates that ultrasonic treatments do not damage the microstructure and permeability of the membrane synthesized by co-sintering at 1300 °C.

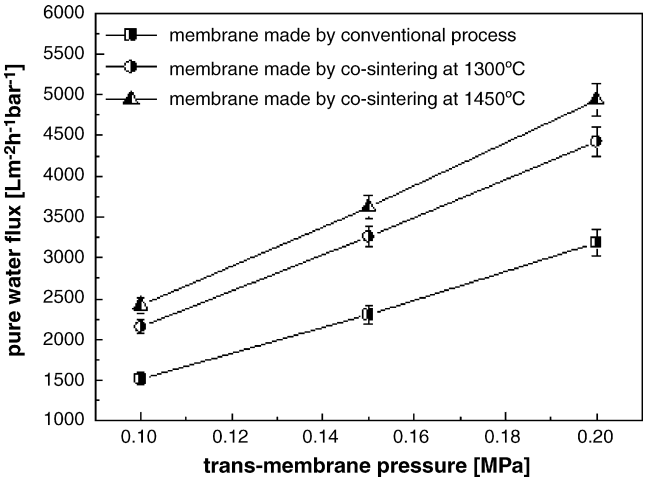

Fig. 9. Pure water flux vs. trans-membrane pressure for bilayer α-Al_2O_3 membranes synthesized by different processes (operating temperature 25 °C).

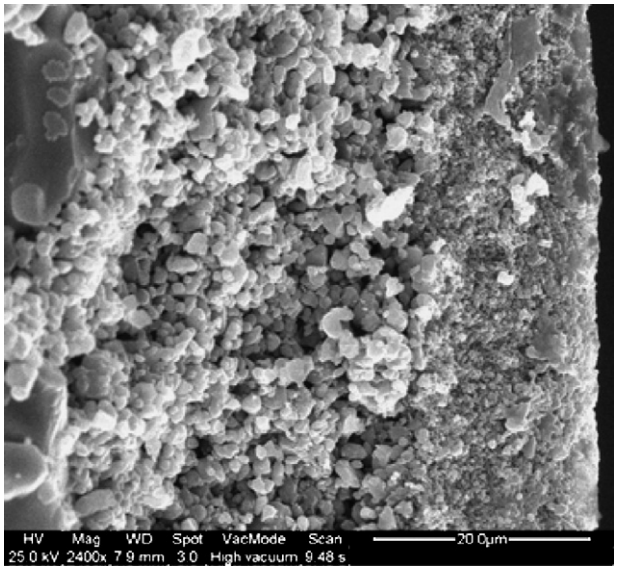

Fig. 10. The cross-section morphology of bilayer α-Al_2O_3 membrane prepared by conventional process.

3.4. Filtration performance

To test the separation performance of the bilayer membrane prepared by the co-sintering process, we produced 19-channel bilayer α-alumina membranes (0.20 μm in average pore size and 0.5 m in length) by co-sintering at 1300 °C. Another α-alumina membrane with similar structure (19-channels, bilayer, 0.20 μm in average pore size and 0.5 m in length) was prepared with the conventional method for comparison. The both membranes were total barriers to the $CaCO_3$ suspension. Filtrations were carried out on the both membranes with the same $CaCO_3$ suspension under the same hydraulic condition.

Table 1
Average pore size and PWF values for bilayer α-alumina membrane fabricated by co-sintering at 1300 °C before and after ultrasonic treatments

Times	PWF ($\times 10^3$ Lm^{-2} h^{-1} bar^{-1})	Average pore diameter (μm)
Before ultrasonic treatment	2.15	0.20
Ultrasonic treatment 1	2.20	0.20
Ultrasonic treatment 2	2.13	0.21
Ultrasonic treatment 3	2.10	0.21

Operating temperature 25 °C; trans-membrane pressure 0.1 MPa; ultrasonic vibrations (160 W, 40 KHz) 30 min.

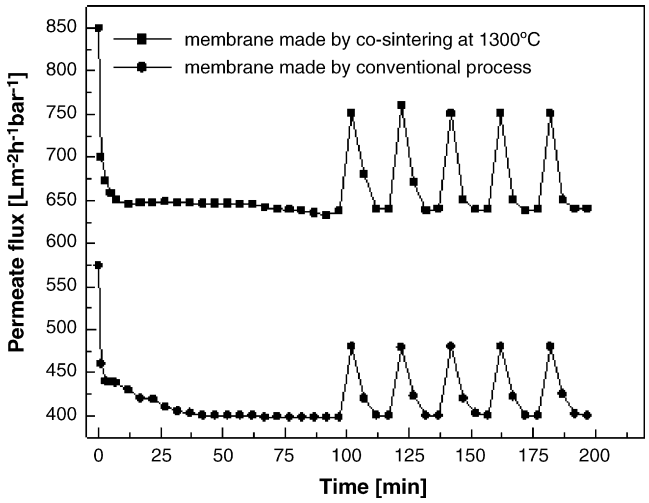

Fig. 11. Filtration results of $CaCO_3$ suspension on 0.20 μm bilayer α-alumina membranes with back-flushing (operating temperature 25 °C, trans-membrane pressure 0.1 MPa, cross-flow velocity 3 m s^{-1}, back-flushing pressure 0.5–0.6 MPa and duration 5 s).

Permeate flux decline and recovery after back-flushing curves are shown in Fig. 11. It reveals that the membrane treated by co-sintering process has a higher steady-state permeate flux than the membrane prepared by conventional process. It is also noticed that the permeate fluxes improve after each back-flushing process and then decline to a similar steady permeate flux. After the filtration test, the equipment and the membrane were cleaned with 0.05 wt.% nitric acid at 70 °C for 2 h. Then the membranes were flushed with pure water and the PWF of the used membrane was measured again. The PWF of both membranes after cleaning was restored almost to a level as high as that of the clean membranes. These results can verify again that the bilayer α-alumina membrane prepared by the co-sintering process can withstand high back-flushing pressure without damage during filtration.

4. Conclusions

This work shows that it is possible to fabricate tubular bilayer α-alumina membranes by the co-sintering process. Too large shrinkage mismatch between two membrane layers, which occurs when co-sintering at 1450 °C, causes many defects such as cracks and big pores. Moderate shrinkage mismatch existed when co-sintering at 1300 °C, which can bring compressive stress in the sub-layer membrane, is beneficial to the whole co-sintering process. Ultrasonic treatments do not damage the microstructure and the permeability of the bilayer membrane obtained by co-sintering at 1300 °C. The filtration of the $CaCO_3$ suspension shows that the membrane treated by co-sintering has

a higher steady permeate flux than the membrane prepared by conventional process and can withstand a high back-flushing pressure.

The co-sintering process simplifies the preparation of bilayer tubular membranes, which could cut the costs and time of production greatly. The bilayer membrane developed in this study may be applied either as a microfiltration membrane or as an intermediate membrane for supporting ultrafiltration membranes.

This preliminary investigation was mainly focused on the optimization of co-sintering temperature. Further study is needed on the influence of membrane layer thickness during co-sintering and the co-sintering of membrane layers with different compositions.

Acknowledgements

This work was supported by the National Basic Research Program of China (no. 2003CB615707), the National Nature Science Foundation of China (no. 20436030) and the Natural Science Research Plan of Jiangsu Universities (no. 04KJB530043).

References

[1] A.J. Burggraaf, Fundamentals of Inorganic Membrane Science and Technology, Elsevier Science B.V., 1996.
[2] K. Lindqvist, E. Liden, Preparation of alumina membranes by tape casting and dip coating, J. Eur. Ceram. Soc. 17 (1997) 359–366.
[3] J. Liu, W. Riess, Ch. Munch, G. Ziegler, Development of a co-firing technique for the production process of ceramic ultrafiltration membranes, in: Proceedings of 7th Conference and Exhibition of the European Ceramic Society, Belgium, September 9–13, 2001.
[4] J. de Jong, N.E. Benes, G.H. Koops, M. Wessling, Towards single step production of multi-layer inorganic hollow fibers, J. Membrane Sci. 239 (2004) 265–269.
[5] A. Rafferty, Y. Gun'ko, R. Raghavendra, An investigation of co-fired varistor-ferrite materials, J. Eur. Ceram. Soc. 24 (2004) 2005–2013.
[6] T.L. Nguyen, K. Kobayashi, T. Honda, Preparation and evaluation of doped ceria interlayer on supported stabilitized zirconia electrolyte SOFCs by wet ceramic processes, Solid State Ionics 174 (2004) 163–174.
[7] W.T. Bao, Q.B. Chang, G.Y. Meng, Effect of NiO/YSZ compositions on the co-sintering process of anode-supported fuel cell, J. Membrane Sci. 259 (2005) 103–109.
[8] W.Q. Jin, S.G. Li, P. Huang, N.P. Xu, J. Shi, Preparation of an asymmetric perovskite-type membrane and its oxygen permeability, J. Membrane Sci. 185 (2001) 237–243.
[9] A.F.M. Leenaars, A.J. Burggraaf, The preparation and characterization of alumina membranes with ultra-fine pores: Part 3. The permeability for pure liquids, J. Membrane Sci. 24 (1985) 245–260.
[10] R. Sondhi, Y.S. Lin, F. Alvarez, Crossflow filtration of chromium hydroxide suspension by ceramic membranes: fouling and its minimization by backpulsing, J. Membrane Sci. 174 (2000) 111–122.
[11] Y.J. Zhao, J. Zhong, H. Li, N.P. Xu, J. Shi, Fouling and regeneration of ceramic microfiltration membranes in processing acid wastewater containing fine TiO_2 particles, J. Membrane Sci. 208 (2002) 331–341.
[12] R.K. Bordia, R. Raj, Sintering behavior of ceramic films constrained by a rigid substrate, J. Am. Ceram. Soc. 68 (6) (1985) 287–292.
[13] T.J. Garino, H.K. Bowen, Kinetics of constrained-film sintering, J. Am. Ceram. Soc. 73 (2) (1990) 251–257.
[14] G.W. Scherer, T. Garino, Viscous sintering on a rigid substrate, J. Am. Ceram. Soc. 68 (4) (1985) 216–220.
[15] D.S. Smith, A. Smith, The effect of differential shrinkage in ceramic bonding, J. Mater. Sci. Lett. 5 (1986) 349–352.
[16] P.Z. Cai, D.J. Green, G.L. Messing, Constrained densification of alumina/zirconia hybrid laminates. 1. Experimental observations of processing defects, J. Am. Ceram. Soc. 80 (8) (1997) 1929–1939.
[17] S. Ho, C. Hillman, F.F. Lange, Z. Suo, Surface cracking in layers under biaxial, residual compressive stress, J. Am. Ceram. Soc. 78 (9) (1995) 2353–2359.
[18] T.X. Liang, J.G. Zhu, B. Yang, B.Z. Zhang, X.L. Peng, Sintering stresses in co-sintered AlN/W multilayer substrates, J. Chinese Ceram. Soc. 26 (3) (1998) 286–291 (in Chinese).
[19] S.C. Thompson, A. Pandit, N.P. Padture, Stepwise-graded Si_3N_4–SiC ceramics with improved wear properties, J. Am. Ceram. Soc. 85 (8) (2002) 2059–2064.
[20] W.D. Kingery, H.K. Bowen, D.R. Uhlmann, Introduction to Ceramics, Wiley-Interscience, New York, 1975.
[21] P. Wang, P. Huang, N.P. Xu, J. Shi, Y.S. Lin, Effects of sintering on properties of alumina microfiltration membranes, J. Membrane Sci. 155 (1999) 309–314.